www.czasopisma.pan.pl PAN POLSKA AKADEMIA NAUK www.journals.pan.pl

Arch. Metall. Mater. **69** (2024), 1, 99-102

DOI: https://doi.org/10.24425/amm.2024.147794

MINHA PARK[1], GANG HO LEE[1,2], GWANGJOO JANG[1], HYOUNG-CHAN KIM[1], BYOUNGKOO KIM[1], BYUNG JUN KIM[1*]

THE EFFECTS OF POST WELD HEAT TREATMENT ON MICROSTRUCTURE AND MECHANICAL PROPERTIES OF API X70 LINEPIPE USING SUBMERGED ARC WELDING

API X70 steel requires high strength and toughness for safety in extreme environments like high pressure and low temperature. Submerged Arc Welding (SAW) is effective for manufacturing thick steel pipes. However, the welding heat input during SAW alters the microstructure and mechanical properties of the heat affected zone (HAZ). Therefore, investigating the correlation between microstructure and mechanical properties in welded X70 pipes is important to address potential degradation of HAZ and weld metal (WM). In this study, post weld heat treatment (PWHT) was performed to improve mechanical properties of HAZ and WM and to reduce residual stress caused by the welding process. We performed PWHT at 640°C for 15 hours and followed by air cooling. After heat treatment, we observed the microstructure through OM and SEM analysis, and investigated the mechanical properties through tensile test, hardness test, and Charpy impact test.

Keywords: API X70; Post weld heat treatment (PWHT); Submerged Arc Welding (SAW); mechanical properties

1. Introduction

As the demand for oil and gas rises, the oil and gas industry is increasingly focusing on developing facilities in deep-sea environments. In offshore plant industries, API steel is commonly used for pipelines, which are typically large and thick. Specifically, X70 steels are sought after for their high strength and toughness, essential for ensuring safety and reliability in extreme conditions such as high pressure and low temperature [1,2]. Presently, research efforts are concentrated on enhancing the strength, toughness, and resistance of these steels to withstand high pressure and low temperature environments. Especially, it is important to secure low ductile-brittle transition temperature (DBTT) under extremely environments since the body-centered cubic (BCC) materials such as API X70 have decreasing toughness with decreasing temperature [3,4].

In addition, a welding process such as SAW is an effective method for manufacturing thick steel pipes for various plant industries. However, the welding heat input during SAW causes changes to the microstructure and mechanical properties of the HAZ. These microstructural changes can negatively impact the mechanical properties, including strength, ductility, and impact toughness. In general, high strength steels like X70 undergo PWHT to reduce residual stress and dislocation density from the welding process and improve their mechanical properties [5,6]. This study aimed to investigate the influence of PWHT on the microstructure and mechanical properties of welded X70 pipes. After PWHT, the correlation between the microstructure and mechanical properties of welded X70 pipes was investigated.

2. Experimental

The chemical compositions of base metal (BM) and weld metal (WM) used of API X70 in this study are shown TABLE 1. The Submerged Arc Welding (SAW) process was employed with a double V-groove configuration over three passes. The welding parameters included a current ranging from 460-870 A, voltage between 33-39V, and a welding speed of 0.4-0.7 cm/min. To alleviate stress and eliminate internal hydrogen, a PWHT was conducted at a temperature of 640°C for a duration of 15 hours.

Tensile testing was performed at a strain rate of 10^{-3}/s using sub-sized plate-type specimens measuring 6.4 mm in gauge length, 2.5 mm in width, and 2 mm in thickness. The yield

[1] ENERGY SYSTEM GROU, KOREA INSTITUTE OF INDUSTRIAL TECHNOLOGY, 46938, BUSAN, REPUBLIC OF KOREA
[2] PUKYONG NATIONAL UNIVERSITY, DEPARTMENT OF MATERIALS SCIENCE AND ENGINEERING, 48513, BUSAN, REPUBLIC OF KOREA

* Corresponding author: jun7741@kitech.re.kr

TABLE 1

Chemical composition of base metal (BM) and weld metal (WM) of API X70

	C	Si	Mn	P	S	Cr	Ni	Fe
Base metal (BM)	0.0612	0.236	1.614	0.0093	0.0012	0.133	0.079	Bal.
Weld metal (WM)	0.06	0.31	1.25	0.017	0.011	—	—	Bal.

strength was determined using the 0.2% offset stress method, while elongation was measured by tracking the travel distance of the crosshead. Vickers hardness tests were conducted with a 4.903 N load applied for 10 seconds. The hardness data represents an average of seven indentations, excluding the minimum and maximum values.

Charpy impact tests were carried out using an automatic ZWIC impact test machine with a capacity of 750 J, ranging from –140°C to 20°C. The Charpy impact specimens were prepared according to ASTM E23 standards, measuring 10 mm × 10 mm × 55 mm, featuring a V-notch with a depth of 2 mm at a 45° angle. The load-displacement curve was obtained using an instrumented impact pendulum device with a nominal impact velocity of 5.424 m/s.

For microstructure characterization, a scanning electron microscope (SEM) and electron backscattering diffraction (EBSD) analysis were performed using a JEOL FE-SEM 7200F. The microstructure samples underwent mechanical grinding with SiC paper, followed by polishing with 3 µm and 1 µm diamond paste. Etching was conducted using a 3% nital solution for 30 seconds. Additionally, specimens were prepared for EBSD analysis using 0.25 µm diamond paste colloidal silica during the final polishing stage.

3. Results and discussion

Fig. 1 shows the microstructure of X70 steels base metal (BM), heat affected zone (HAZ), and weld metal (WM) before and after PWHT. Prior to PWHT, the microstructure of the BM consisted primarily of complex microstructures such as granular bainite (GB) and acicular ferrite (AF) (Fig. 1a). In the HAZ, the welding heat input resulted in the formation of complex microstructures, including martensite-austenite (MA) and GB in both the fine-grained heat-affected zone (FGHAZ) and the coarse-grained heat-affected zone (CGHAZ) (Fig. 1b-c). The microstructures of the WM were characterized by AF and grain boundary allotriomorphic ferrite (depicted as white regions) (Fig. 1d) [7]. After heat treatment, the microstructure of the BM showed the presence of AF, GB, and polygonal ferrite (PF), with partial recrystallization occurring in the austenite-ferrite two-phase region due to the heat treatment process (Fig. 1e). In the HAZ microstructure, secondary phase decomposition of martensite and spheroidization of cementite carbide were observed (Fig. 1f-g) [7]. Furthermore, in the WM microstructure, a reduction in grain boundary allotriomorphic ferrite was observed (Fig. 1h).

Fig. 2 shows the tensile properties and hardness properties of welded X70 steels before and after PWHT. Before PWHT, the yield strength (YS) and tensile strength (TS) of BM were about 543 MPa and 606 MPa, respectively in Fig 2a. After heat treatment, the strength of the BM showed a tendency to decrease compared to the strength before heat treatment. Conversely, the elongation of the BM slightly increased after heat treatment. Regarding the WM, its yield strength and tensile strength were measured at 566 MPa and 627 MPa, respectively, which were higher than those of the BM. After heat treatment, the tensile properties of the WM were similar to the results obtained for the BM. However, the strength decreased and the elongation increased. Fig. 2b shows the Vickers hardness results of welded

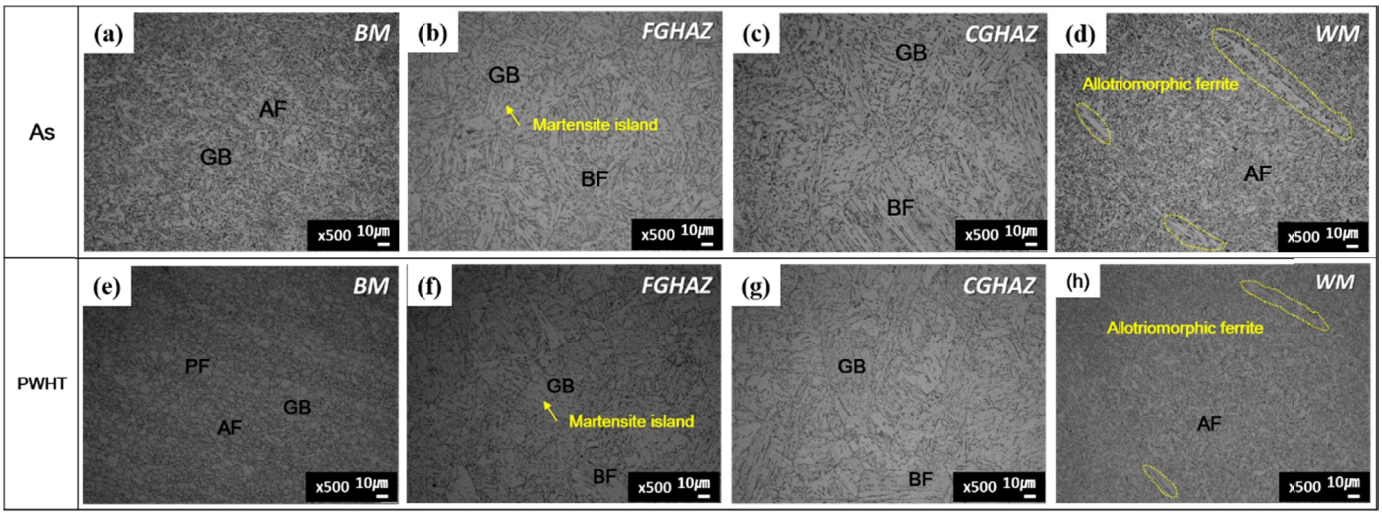

Fig. 1. Microstructure of welded API X70 before and after PWHT: (a) BM (before PWHT), (b) FGHAZ (before PWHT), (c) CGHAZ (before PWHT), (d) WM (before PWHT), (a) BM (after PWHT), (b) FGHAZ (after PWHT), (c) CGHAZ (after PWHT), and (d) WM (after PWHT)

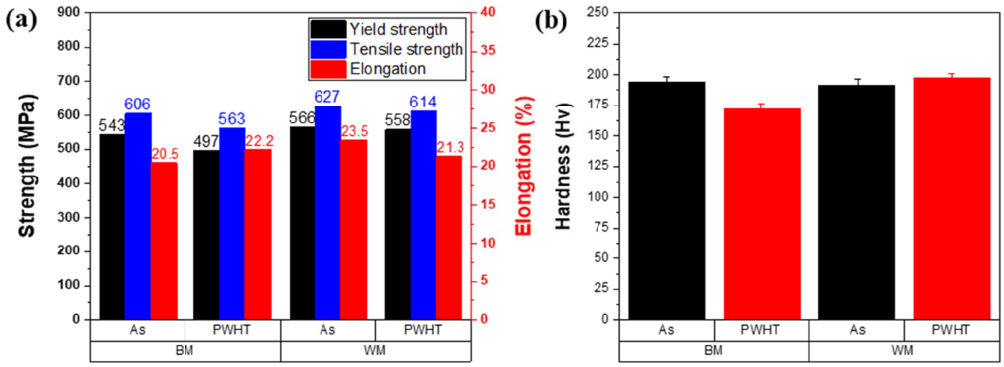

Fig. 2. The results of tensile test and hardness test before and after PWHT: (a) Tensile properties and (b) Hardness properties

X70 steels before and after PWHT. The hardness of BM was measured to be about 198 Hv before heat treatment, and the hardness value decreased to about 175 Hv after heat treatment. After heat treatment, the hardness value decreased by increasing the fraction of PF and GB with excellent ductility. In the case of the WM, the hardness measurement was approximately 176 Hv before heat treatment. However, after heat treatment, the hardness increased to around 178 Hv due to a decrease in the fraction of allotriomorphic ferrite.

The absorbed energy vs. test temperature curves for welded X70 steels was shown in Fig. 3a. The X70 steel, with its body-centered cubic (BCC) structure, exhibited the typical ductile-to-brittle transition (DBT) behavior. In the case of the BM and HAZ, the DBTT shifted to higher temperatures, while the upper shelf energy (USE) decreased after PWHT. However, in the WM, the DBTT after PWHT shifted to lower temperatures, and the USE increased, contrary to the behavior observed in the BM and HAZ. Comparing the impact properties before and after heat treatment, the DBTT of the WM decreased by 16°C, while the USE increased by 25 J. This indicates an improvement in the impact properties of the WM, while the impact properties of the BM and HAZ were reduced. Generally, failure in welded structures occurs in weaker regions such as the WM. Therefore, PWHT is valuable for enhancing the impact properties of the WM. Fig. 3b shows the load-displacement curves obtained by the instrumented Charpy impact test at low temperature (−40°C) before and after PWHT of WM. The crack initiation energy (E_i) and crack propagation energy (E_p) were calculated by determining the areas beneath the load-displacement curves based on the maximum load (P_{max}) value. In Fig. 3b, the P_{max} value of the WM increased from 68.1 kN to 71.9 kN after PWHT. Additionally, the crack initiation energy (E_i) of the WM increased from approximately 38.4 J before PWHT to about 83.2 J after PWHT, representing an increase from 50.5% to 53.1%. However, the crack propagation energy (E_p) of the WM decreased from about 37.6 J before PWHT to 73.8 J after PWHT, indicating a decrease from 49.5% to 46.9%.

Fig. 4 presented the inverse pole figure (IPF) and grain boundary (GB) maps obtained from electron backscattering diffraction (EBSD) analysis of the cross-sectional area of fractured Charpy impact specimens at –40°C for the WM before and after PWHT. Notably, the crack propagation in the specimen after heat treatment (Fig. 4b) exhibited more deflection compared to the specimen before heat treatment (Fig. 4a). In the case of the WM before heat treatment, the main crack tended to propagate more easily along the coarsed allotriomorphic ferrite phase, particularly where high-angle grain boundaries (HAGBs) of 15° or more were present (Fig. 4a). However, after heat treatment (Fig. 4b), the main crack was deflected due to the interference of fine grains and the AF phase [2,8]. This deflection of the crack path was attributed to the random arrangement of fine AF phases. Consequently, the absorbed energy after heat treatment increased, reflecting the disturbance caused by these randomly distributed fine AF phases.

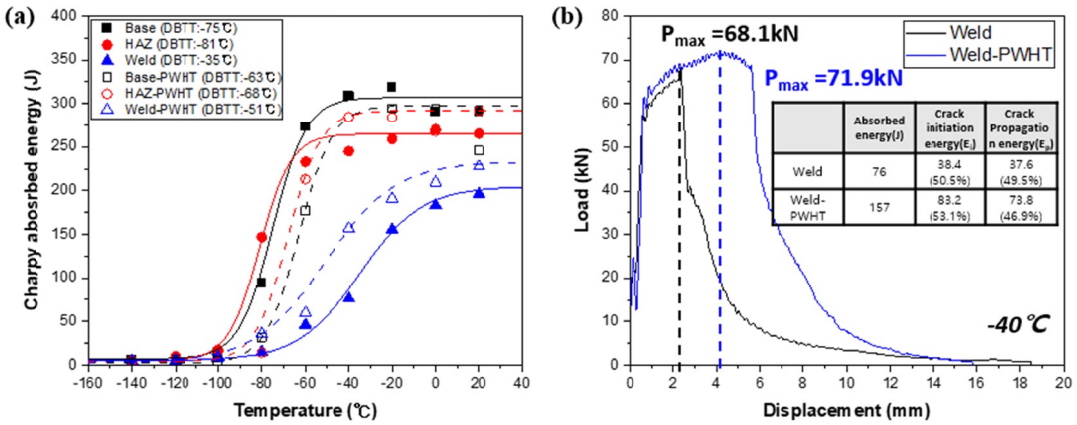

Fig. 3. Charpy impact property of X70 steel before and after PWHT: (a) The absorbed energy vs. test temperature curves and (b) Load-Displacement curves obtained by instrumented Charpy impact test at −40°C

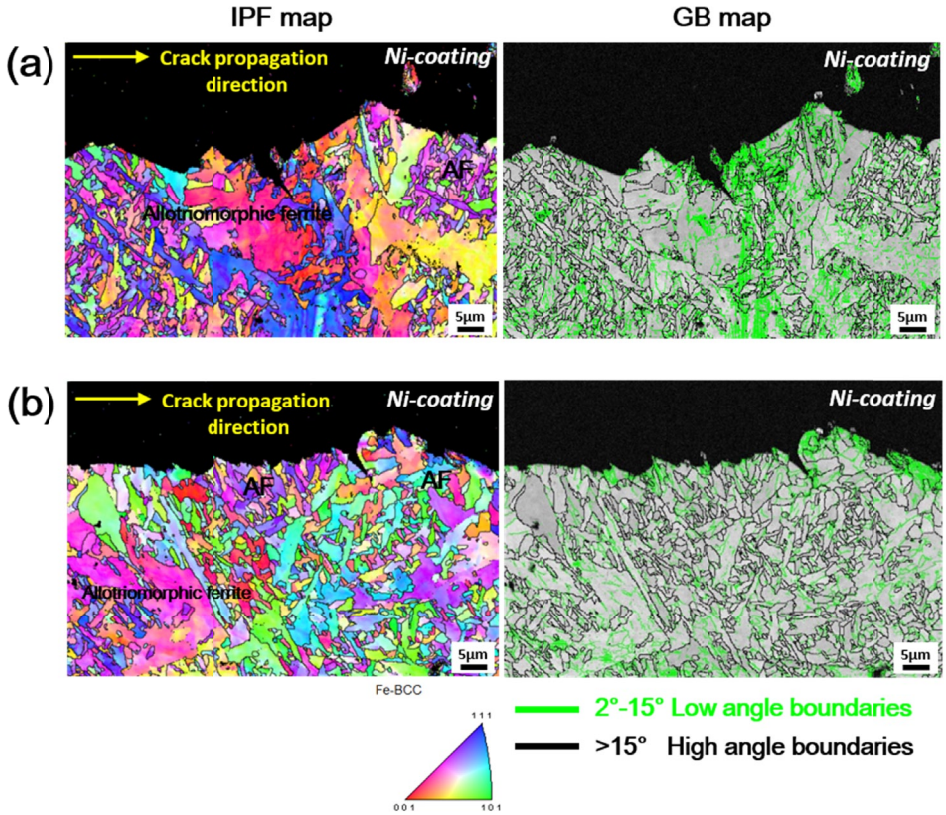

Fig. 4. EBSD IPF and GB maps of the cross-sectional area of the fractured Charpy impact specimens at −40°C of the WM before and after PWHT: (a) before PWHT and (b) after PWHT

4. Conclusions

In this study, the correlation between the microstructure and mechanical properties of welded X70 pipes was investigated after PWHT. The microstructure of BM and HAZ was mainly composed of complex microstructures such as GB, AF and BF, and that of WM was consisted of AF and allotriomorphic ferrite. In the WM, the DBTT after PWHT is shifted to lower temperatures and USE increased, contrary to the result of the BM and HAZ. Also, the main crack was deflected due to the interference of fine grain and the AF phase. As a result, the absorbed energy after heat treatment increased due to the disturbance of randomly arranged fine AF phases.

Acknowledgments

This study was supported by the R&D Program of the "the International joint technology development project (P0019244, Development of eco-friendly high-performance forged parts manufacturing technology based on AI intelligent plastic processing system).

REFERENCES

[1] H.L. Kim, S.H. Bang, J.M. Choi, N.H. Tak, S.W. Lee, S.H. Park, Effect of rolling and coiling temperatures on Microstructure and Mechanical Properties of Medium-Carbon Pipeline Steel. Met. Mater. Int. **26**, 1757-1765 (2020).

[2] S.Y. Shin, B. Hwang, S. Lee, N.J. Kim, S.S. Ahn, Correlation of Microstructure and Charpy impact Properties in API X70 and X80 Line-pipe Steels. Mater. Sci. Eng. A. **458** (1-2), 281-289 (2007).

[3] J.-H. Kim, S.-W. Choi, D.-H. Park, J.-M. Lee, Charpy Impact Properties of Stainless Steel Weldment in Liquefied Natural Gas Pipelines: Effect of Low Temperatures. Mater. Des. **65**, 914-922 (2015).

[4] S.-W. Lee, S.-I. Lee, B. Hwang, Effect of Bainitic Microstructure on Low-Temperature Toughness of High-Strength API Pipeline Steels. Korean. J. Met. Mater. **58** (5), 293-303 (2020).

[5] H. Alipooramirabad, A. Paradowska, S. Nafisi, M. Reid, R. Ghomashchi, Post-weld Heat Treatment of API 5L X70 High Strength Low alloy Steel Welds. Materials **13** (24), 5801-5824 (2020).

[6] D.-H. Yang, G.-S. Ham, S.-H. Park, K.-A. Lee, Effect of stress relieving heat treatment on tensile and impact toughness properties of AISI 316L alloy manufactured by selective laser melting process. J. P owder Mater. **28** (4), 301-309 (2021).

[7] W.S.H. W. Muda, N.S.M. Nasir, S. Mamat, S. Jamian, Effect of Welding Heat Input on Microstructure and Mechanical Properties at Coarse Grain Heat Affected Zone of ABS grade a Steel. Materials. ARPN J. Eng. Appl. Sci. **10** (20), 9487-9495 (2015).

[8] H.K. Sung, S.S. Sohn, S.Y. Shin, K.S. Oh, S. Lee, Metal. Effects of Oxides on Tensile and Charpy Impact Properties and Fracture Toughness in Heat Affected Zones of Oxide-Containing API X80 Linepipe Steels. Mater. Trans. A. **45**, 3036-3050 (2014).